IOPscience iopscience.iop.org

Home Search Collections Journals About Contact us My IOPscience

Investigating dynamical tunnelling in open quantum dots by means of a soft-walled microwave-cavity analogue

This article has been downloaded from IOPscience. Please scroll down to see the full text article.

2005 J. Phys.: Condens. Matter 17 L191

(http://iopscience.iop.org/0953-8984/17/19/L03)

View the table of contents for this issue, or go to the journal homepage for more

Download details:
IP Address: 129.252.86.83
The article was downloaded on 27/05/2010 at 20:43

Please note that terms and conditions apply.

INSTITUTE OF PHYSICS PUBLISHING JOURNAL OF PHYSICS: CONDENSED MATTER

J. Phys.: Condens. Matter **17** (2005) L191–L198 doi:10.1088/0953-8984/17/19/L03

LETTER TO THE EDITOR

Investigating dynamical tunnelling in open quantum dots by means of a soft-walled microwave-cavity analogue

Y-H Kim[1], U Kuhl[1], H-J Stöckmann[1] and J P Bird[2]

[1] Fachbereich Physik der Philipps-Universität Marburg, Renthof 5, D-35032 Marburg, Germany
[2] Department of Electrical Engineering, University at Buffalo, Buffalo, NY 14260-1920, USA

E-mail: ulrich.kuhl@physik.uni-marburg.de

Received 12 April 2005, in final form 12 April 2005
Published 29 April 2005
Online at stacks.iop.org/JPhysCM/17/L191

Abstract

We investigate the signatures of dynamical tunnelling in open quantum dots, by implementing a soft-walled microwave cavity as a novel analogue system. We explore the evidence for dynamical tunnelling by studying the evolution of the wavefunction phase as a function of frequency and show evidence for evanescent coupling to isolated orbits, including the existence of 'dirty' states in the wavefunction that are generated from a degenerate pair of 'clean' states when they are degraded by their tunnelling interaction. Our investigations provide a useful analogue of quantum transport in open quantum dots, and demonstrate the importance of dynamical tunnelling that arises from the mixed classical dynamics that is inherent to these structures.

In recent years, semiconductor quantum dots have been widely explored as a versatile system for studying the signatures of classical chaos in quantum mechanics. The conductance of such dots exhibits mesoscopic fluctuations at low temperatures, which provide a powerful tool for analysing the connection of quantum transport to the underlying classical dynamics of the system [1–6]. Among the issues that have been revealed in these studies include measurable transport results due to wavefunction scarring, whose characteristics depend strongly on the nature of the environmental coupling to the quantum dot [5], and evidence for self-similar structure in the magneto-conductance [3, 4]. More recent work [7] has even connected the unique features of quantum transport in open dots to the existence of robust 'pointer states', whose role has been emphasized in theoretical discussions of the classical-to-quantum transition [8].

In many studies to date [1, 2], it has been popular to analyse the statistical properties of the conductance fluctuations in open dots by making a simple assumption that these structures give rise to fully chaotic (hyperbolic) classical dynamics [1, 2]. More recently [3, 4], however, there

 © 2005 IOP Publishing Ltd Printed in the UK

has been a growing appreciation that, due to the soft-walled nature of the confining profile in these dots [9], and the presence of the lead openings that connect them to their reservoirs [10], the relevant classical dynamics in these systems is in fact mixed (non-hyperbolic). This important difference in the structure of the classical phase space leads to very significant implications for the quantum mechanical properties of the dots. In one study, in particular, it was argued that the appearance of wavefunction scarring in open dots can be related to the dynamical tunnelling of electrons, to access isolated orbits in phase space that are decoupled from the quantum-dot leads [6]. This process is distinct from tunnelling in the usual sense, since the 'tunnel barrier' is provided by the existence of classically forbidden regions of phase space, rather than any potential barrier [11–13].

Recently, we have explored the use of microwave cavities, as an analogue system for the investigation of transport in open quantum dots. Such investigations are made possible by the equivalence, for a two-dimensional system, of the Schrödinger and Helmholtz equations, according to which a measurement of the electric field within the cavity is analogous to the wavefunction in the corresponding quantum dot [14]. Our previous investigations of this system have focused on the use of hard-walled cavities to mimic quantum-dot transport [15]. For a more quantitative comparison, however, in this letter we report on the implementation of a soft-walled microwave resonator in which the signatures of dynamical tunnelling in transport are investigated [16]. Unlike the situation in quantum dots, where only the quantum mechanical transmission probability of electrons can be probed in experiment, in our soft-walled microwave resonator we are able to investigate evidence for dynamical tunnelling by studying the evolution of the wavefunction phase. Our study confirms the existence of dynamical tunnelling in soft-walled quantum dots, showing evidence for evanescent coupling to isolated orbits, including the existence of 'dirty' states [17] in the wavefunction that are generated from a degenerate pair of 'clean' states when they are degraded by their tunnelling interaction.

In a microwave resonator with parallel top and bottom plates, the electric field $E(x, y, z)$ points from top to bottom in the z direction for the lowest modes, the transverse magnetic modes. In the three-dimensional Helmholtz equation for $E(x, y, z)$, the z dependence can be separated out, resulting in a two-dimensional Helmholtz equation for $E(x, y)$

$$\left[-\Delta_{xy} + \left(\frac{n\pi}{d}\right)^2\right] E(x, y) = k^2 E(x, y), \tag{1}$$

where k is the wavenumber, d the height of the resonator, and n the k_z quantum number. For $n = 0$ this is equivalent to the stationary Schrödinger equation for a two-dimensional billiard with Dirichlet boundary condition, which has been used in numerous experiments [14]. For $n = 1$, however, the additional term can be used to mimic a potential $V(x, y)$ by putting

$$d(x, y) \sim \frac{1}{\sqrt{V(x, y)}}. \tag{2}$$

The approach is not exact, since the separation of the z component works for constant d only, but as long as the potential variation is small on the scale of the wavelength the error terms can be neglected.

Figure 1(a) shows a sketch of the resonator used together with its height profile. The minimum distance between the top and bottom plate was $d_{\min} = 6.3$ mm outside the resonator increasing gradually to $d_{\max} = 16.7$ mm in the bottom of the resonator. Due to a small and unavoidable misalignment of the top plate there were variations of the height over the area of the resonator of up to 0.9 mm. The corresponding potential was constant in the bottom of the dot and increased quadratically close to the boundaries, both in the vertical and perpendicular directions as well as along the diagonals; see figure 1(b). Such potential shapes are typical for quantum dots realized by remote surface gates [18].

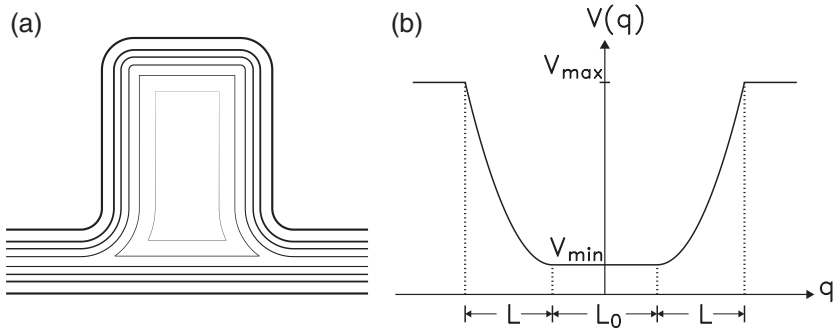

Figure 1. (a) Height profile of the resonator. The top is 10.4 mm above the bottom; between neighbouring contour lines there is a height difference of 2.08 mm. (b) Corresponding potential $V(q)$ along a cut, where $L = 50$ mm, and $L_0 = 60$, 140, and 152 mm for the vertical, horizontal, and diagonal cuts, respectively.

Two antennas A_1 and A_2 serving as source and drain for the microwaves were attached to the leads, which were closed by absorbers. A third antenna A_3 was moved on a quadratic grid of period 5 mm to map out the field distribution within the dot. Details can be found in our previous publications [15, 19]. For $\nu_{\min} = c/(2d_{\max}) = 9$ GHz only the $n = 0$ modes exist. They are not observed, however, since the billiard is open in the xy plane. For $\nu_{\min} < \nu < \nu_{\max} = c/d_{\max} = 18$ GHz the $n = 1$ modes exist as well. Another frequency threshold of relevance is found at $\nu_T = 12.5$ GHz. Below this frequency all $n = 1$ states are bound whereas for higher frequencies the states extend into the attached channels and have thus to be interpreted as resonance states.

Figure 2 shows the modulus of the transmission S_{21} between antenna A_1 in the entrance and antenna A_2 in the exit waveguide, together with the modulus of the reflection S_{33} at the movable antenna A_3 at a fixed position within the billiard in the upper panel. The solid vertical line at 12.5 GHz corresponds to the threshold frequency ν_T where the billiard states can couple to the waveguides. Correspondingly, the transmission is close to zero below this frequency. The vertical dotted lines correspond to a number of selected resonance eigenfrequencies, the corresponding wavefunctions for which are shown in the lower panel. The reflection is dominated by three scar families, two of them associated with the vertical and the horizontal bouncing ball, the third one corresponding to a cross-like structure. The cross-like structure was not observed in our previous experiments on a microwave dot with hard walls. Instead we found a scar with the shape of a loop connecting the entrance and exit ports [19].

A comparison of the reflection and the transmission measurements shows that the bouncing-ball states dominating the reflection contribute only weakly to the transmission. The cross-like structures, on the other hand, exhibit maxima not only in the reflection but also in the transmission spectrum. This is in qualitative agreement with our measurements of a hard-wall microwave dot where we also found that only those states connecting the entrance and exit ports turned out to be relevant for the transport.

In the first panel of figure 3 the eigenfrequencies of all identified vertical bouncing ball states are shown by stars, together with two representative members of the family. Again the vertical line denotes the threshold where the attached channels open. The second and third panels show the respective results for the horizontal bouncing ball and the cross-like scar family.

The eigenfrequencies of the members of the three families can be obtained semiclassically by means of a WKB approximation. In one-dimensional systems with two classical turning

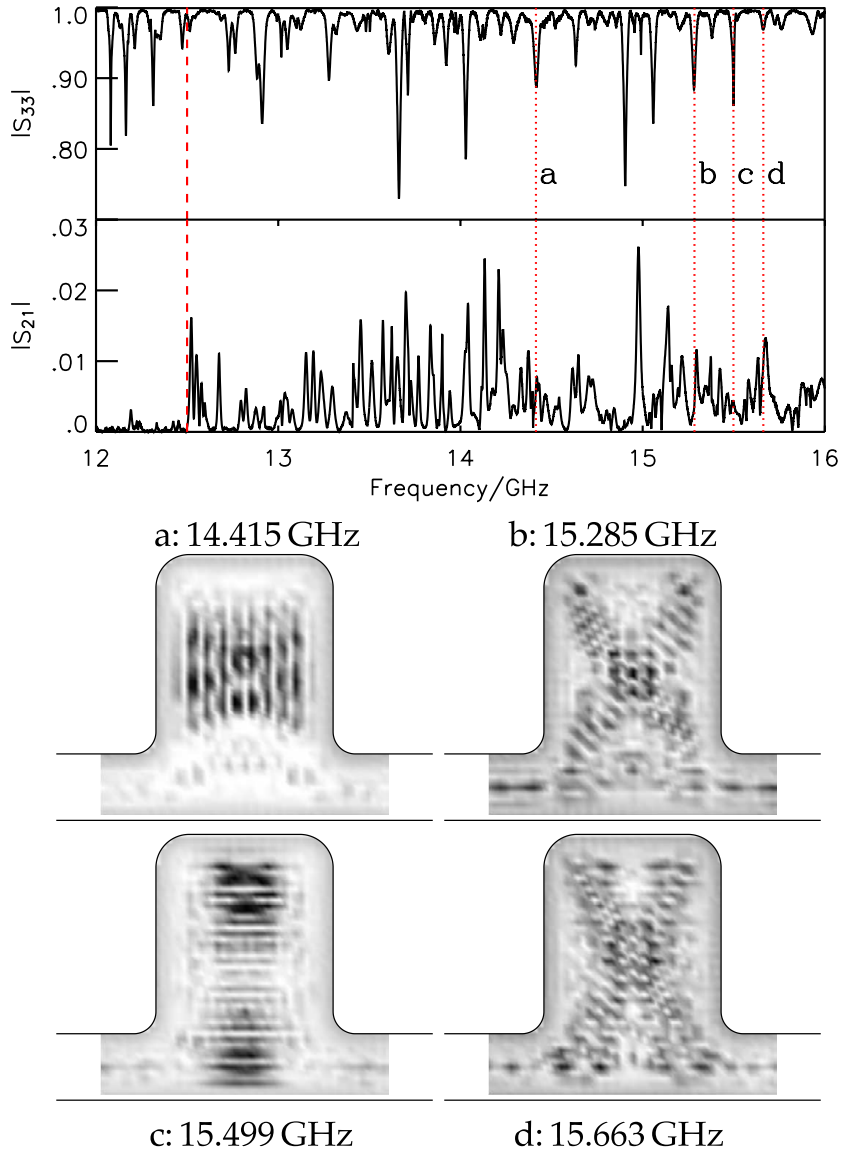

Figure 2. Upper panel: measured reflection spectrum $|S_{33}|$ with antenna A_3 at a fixed position, and transmission spectrum $|S_{21}|$ between antennas A_1 and A_2 in the entrance and the exit port, respectively. Lower panel: wavefunctions for four selected frequencies obtained from the reflection at antenna A_3 as a function of the position.

points q_1, q_2 the action is quantized according to

$$S_n = 2\int_{q_1}^{q_2} p\,\mathrm{d}q = 2\int_{q_1}^{q_2} \sqrt{2m(E_n - V(q))}\,\mathrm{d}q = 2\pi\hbar(n+\tfrac{1}{2}). \tag{3}$$

This gives an implicit expression for the eigenenergy E_n of the nth state. Equation (3) may be applied directly to the scarred structures observed in the experiment. For the two bouncing-ball families a one-dimensional treatment is obviously justified, and the cross-like structure may be looked upon as a superposition of two one-dimensional structures, oriented along the diagonals

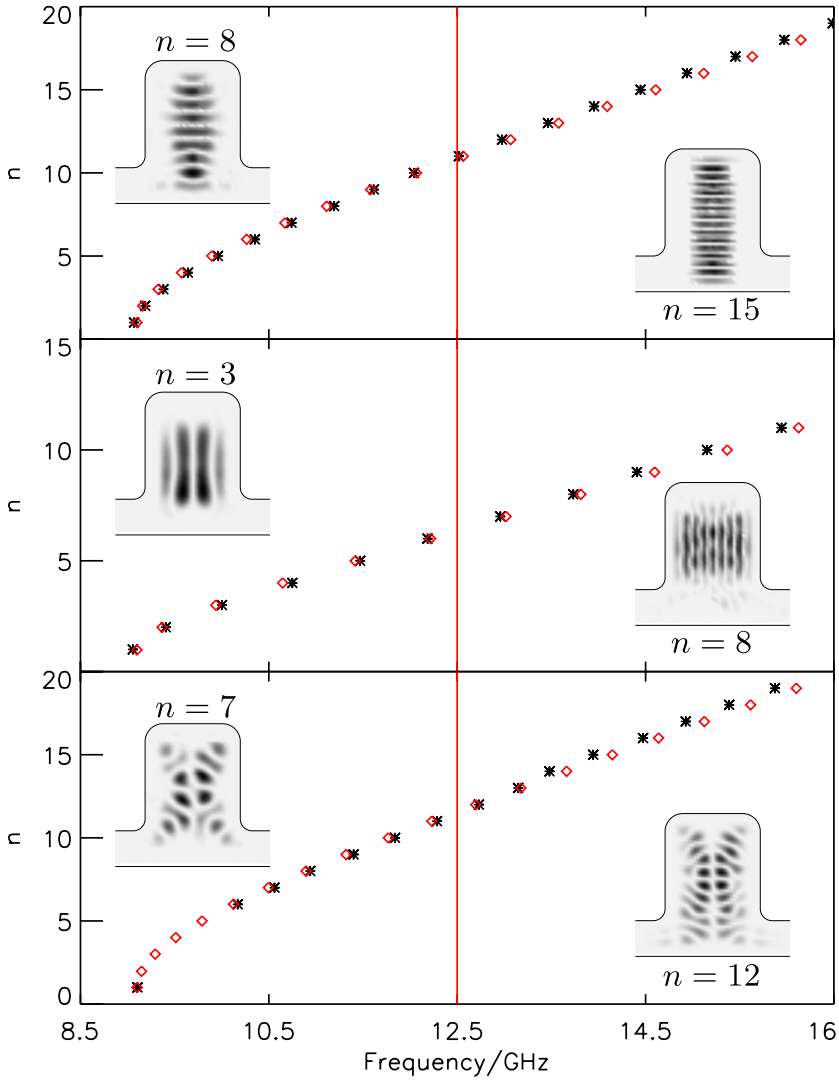

Figure 3. Frequencies of the eigenvalues associated with the three scar families, together with two representative members of the family. Measured values are plotted by stars, calculated ones by diamonds.

of the billiard. For the cross-like structures, the application of the WKB approximation is somewhat questionable above 12.5 GHz, where the states start to extend into the waveguides, but this leads only to small deviations.

Inserting the potential of figure 1 into equation (3), the eigenenergies for all members of the three families can be calculated. The eigenfrequencies are given by $\nu_n = \sqrt{2mE_n}c/(2\pi\hbar)$ and are plotted in figure 3 by diamonds. The overall agreement of the experimental results with the predicted theoretical values is very good. To take possible misalignments between the top and bottom plates into account, a gradient of $d_{\min}$ with an adjustable slope was allowed to improve the agreement (which was good already without this procedure). The resulting variations of $d_{\min}$ were below the experimental uncertainties given above.

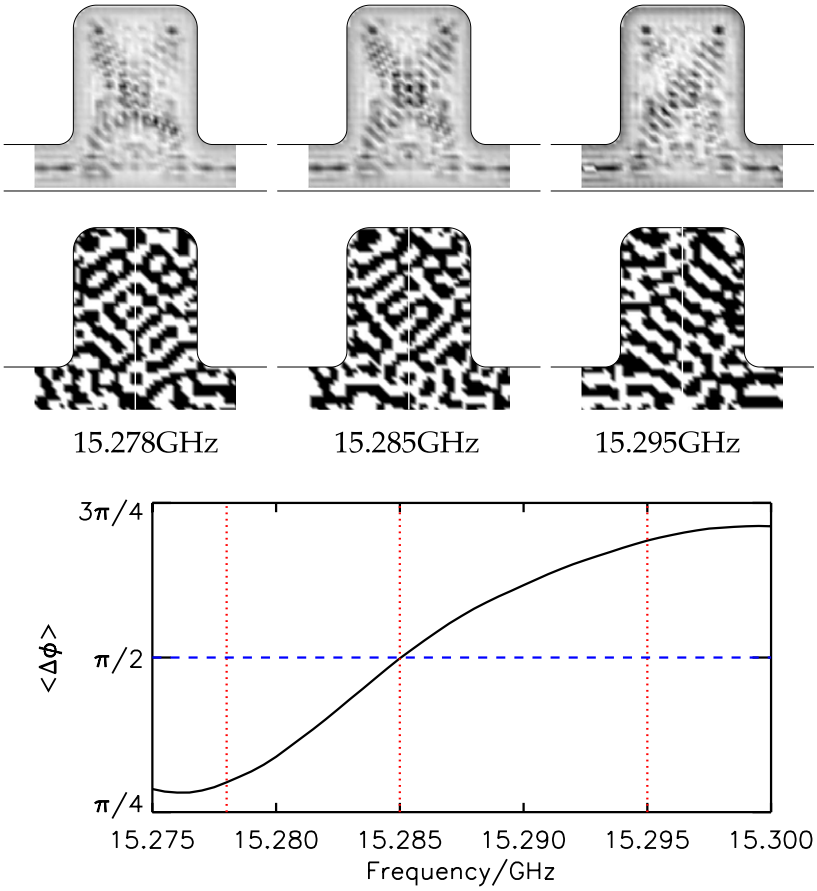

Figure 4. Upper panel: wavefunctions in the low frequency wing, the centre, and the high frequency wing of the resonance, marked by the letter b in figure 2, as obtained from an $|S_{33}|$ measurement. Middle panel: map of the corresponding phases ϕ, obtained from an S_{31} measurement, in a black-white plot. Bottom part: phase asymmetry $\langle\Delta\phi\rangle$ as a function of frequency.

The cross-like structures deserve a separate treatment. Semiclassically, the cross-like state is just an independent superposition of two structures oriented along the diagonals of the dot. Each of these structures corresponds classically to a particle that is injected from one port, then follows the diagonal trajectory, undergoing reflection at the upper corner, before leaving the billiard through the same port. Classically there is no contribution to transport. Figure 2, on the other hand, clearly shows that the cross-like structures do contribute to the transport.

So there must be a quantum mechanical admixture of the states, or, expressed in other words, a dynamical tunnelling coupling of these states. This, however, implies that the originally twofold degenerate states split into doublets, with a symmetric wavefunction associated with the lower, and an anti-symmetric one with the higher energy. An inspection of the spectrum unfortunately does not show any indication of a doublet splitting (see, e.g. the resonances marked by the letters b, d in figure 2). This could not be expected, anyway. In the only previous microwave experiment on chaos-assisted tunnelling, the observed splittings were below 1 MHz [20], much smaller than the line widths observed in the present set-up. Superconducting resonators were essential to resolve such splittings. In the open microwave dot

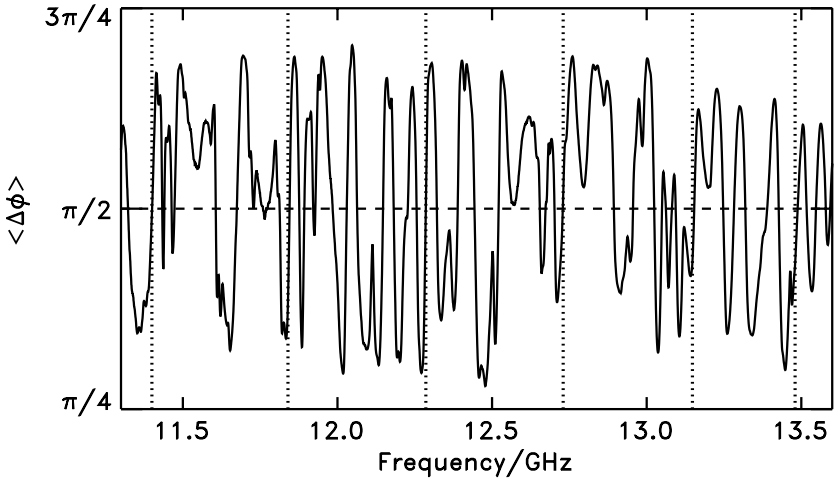

Figure 5. Phase asymmetry $\langle\Delta\phi\rangle$ as a function of frequency. The frequencies corresponding to cross-like wavefunctions are marked by vertical dashed lines.

used in this work, superconducting cavities would not have been of use anyway, since the line widths are limited mainly by the openings, and not by the absorption in the walls.

Fortunately there is an alternative means to obtain direct evidence of dynamical tunnelling, even in cases where the line splitting cannot be resolved. This is illustrated in figure 4. The upper panel shows again the wavefunction at 15.285 GHz, marked by the letter b in figure 2, but in addition the wavefunctions in the lower and higher frequency wings of the resonance are shown as well. There is no noticeable difference between the three patterns. A completely different impression emerges, however, when, in addition, the phases obtained from the transmission S_{31} are also considered. In the middle panel of figure 4 the corresponding phase maps are depicted, demonstrating without any doubt that the wavefunction is symmetric in the low, and anti-symmetric in the high frequency wing of the resonance. To make this even more evident, we calculated the phase asymmetry of the wavefunction via

$$\langle\Delta\phi\rangle = \langle\phi(x, y) - \phi(-x, y)\rangle, \tag{4}$$

where the average is over the area of the dot. $\langle\Delta\phi\rangle$ should be zero for the symmetric case and π for the antisymmetric case. The bottom part of figure 4 shows the phase asymmetry for the 15.285 GHz resonance as a function of frequency. Though the ideal values zero and π are not obtained, a change from symmetric to anti-symmetric behaviour while passing through the resonance is unmistakable. Figure 5 shows the phase asymmetry over a larger frequency range. Frequencies associated with cross-like resonances are marked by vertical dotted lines. For each of these frequencies the phase asymmetry passes through $\pi/2$, from below to above with increasing frequency. We have thus obtained direct evidence of dynamical tunnelling, using nothing but the change of the symmetry properties of the wavefunction upon passing through the resonances.

In conclusion, we have demonstrated a novel manifestation of dynamical tunnelling in a soft-walled microwave resonator. The wavefunction of this system exhibits scarring due to a number of different bouncing orbits, and the eigenfrequencies of these scars were shown to be well described by the WKB approximation. In contrast to previous work, where dynamical tunnelling has been identified by detecting its associated splitting of the eigenspectrum, in this report we obtained direct evidence for the tunnelling process by studying the evolution of the

wavefunction phase as a function of energy (i.e. frequency). This allowed us to identify the conditions for dynamical tunnelling, even though its related level splittings were irresolvable in this system. Our investigations provide a useful analogue of quantum transport in open quantum dots, and demonstrate the importance of dynamical tunnelling that arises from the mixed classical dynamics that is inherent to these structures.

This work was supported by the Deutsche Forschungsgemeinschaft via individual grants. Work at the University at Buffalo is supported by the Department of Energy, the Office of Naval Research and the New York State Office of Science, Technology and Academic Research (NYSTAR).

References

[1] Marcus C M, Rimberg A J, Westervelt R M, Hopkins P F and Gossard A C 1992 *Phys. Rev. Lett.* **69** 506
[2] Chang A M, Baranger H U, Pfeiffer L N and West K W 1994 *Phys. Rev. Lett.* **73** 2111
[3] Taylor R P, Newbury R, Sachrajda A, Feng Y, Coleridge P T, Dettmann C, Zhu N, Guo H, Delage A, Kelly P J and Wasilewski Z 1997 *Phys. Rev. Lett.* **78** 1952
[4] Sachrajda A S, Ketzmerick R, Gould C, Feng Y, Kelly P J, Delage A and Wasilewski Z 1998 *Phys. Rev. Lett.* **80** 1948
[5] Bird J P, Akis R, Ferry D K, Vasileska D, Cooper J, Aoyagi Y and Sugano T 1999 *Phys. Rev. Lett.* **82** 4691
[6] Moura A, Lai Y C, Akis R, Bird J P and Ferry D K 2002 *Phys. Rev. Lett.* **88** 236804
[7] Ferry D K, Akis R and Bird J P 2004 *Phys. Rev. Lett.* **93** 026803
[8] Zurek W H 2003 *Rev. Mod. Phys.* **75** 715
[9] Ketzmerick R 1996 *Phys. Rev.* B **54** 10841
[10] Ferry D K, Akis R and Bird J P 2005 *J. Phys.: Condens. Matter* **17** S1017
[11] Davis M J and Heller E J 1981 *J. Chem. Phys.* **75** 246
[12] Tomsovic S and Ullmo D 1994 *Phys. Rev.* E **50** 145
[13] Frischat S D and Doron E 1998 *Phys. Rev.* E **57** 1421
[14] Stöckmann H J 1999 *Quantum Chaos—An Introduction* (Cambridge: Cambridge University Press)
[15] Kim Y H, Barth M, Stöckmann H J and Bird J P 2002 *Phys. Rev.* B **65** 165317
[16] Lauber H M 1994 Experimenteller Nachweis geometrischer Phasen und Untersuchungen der Wellenmechanik nichtintegrabler Systeme mit Mikrowellenresonatoren *PhD Thesis* Ruprecht-Karls-Universität Heidelberg (see also [14] chapter 2.2.2, p.40ff)
[17] Heller E J 1995 *J. Phys.: Condens. Matter* **99** 2625
[18] Bird J P, Olatona D M, Newbury R, Taylor R P, Ishibashi K, Stopa M, Aoyagi Y, Sugano T and Ochiai Y 1995 *Phys. Rev.* B **52** R14336
[19] Kim Y H, Barth M, Kuhl U and Stöckmann H 2003 Current and vorticity auto correlation functions in open microwave billiards *Let's Face Chaos Through Nonlinear Dynamics (Prog. Theor. Phys. Suppl.)* ed M Robnik, Y Aizawa and Y Kuramoto p 105 (Prog. Theor. Phys. Kyoto)
[20] Dembowski C, Gräf H D, Heine A, Hofferbert R, Rehfeld H and Richter A 2000 *Phys. Rev. Lett.* **84** 867